参赛学生姓名: **Andrea Qian Lei**

中学: **Shanghai High School International Division**

省份: **Shanghai**

国家/地区: **China**

指导老师姓名: **Hui Liao ,Yanjie Zhang**

指导老师单位: **Shanghai High School International Division**
Shanghai Jiao Tong University School of Medicine

论文题目: **Searching for “Smart-and-Sex” Genes — Evolutionary Driver for Neuron and Germ Cell Development in Primates**

Searching for “Smart-and-Sex” Genes — Evolutionary Driver for Neuron and Germ Cell Development in Primates

Andrea Qian Lei

Abstract

Evolution has shaped primates, with humans being one extant branch of the order, to develop two key advanced traits in comparison with lower mammalian species — first, higher intelligence with increased brain size and cortical complexity; and second, a more enhanced reproductive system. Despite their functional and morphological differences, it has become increasingly recognized that the brain and testis, among all the organs of the human body, exhibit the most similar gene expression pattern. Whether there are any “smart-and-sex” genes that drive the evolution of these advanced traits in primates remains an enigma.

In this study, I systematically analyzed multiple publicly available genomic and transcriptomic databases and identified a group of candidate “smart-and-sex” genes. These genes emerged after the primate-rodent split during evolution, and exhibit a significantly higher expression in neural progenitor cells at the peak of human brain development (0-1 year newborn) as well as in male testicular progenitor cells (age 13 and above). To validate, I performed an *in vitro* analysis to examine the impact of these genes on cortical neurogenesis. The data showed that expression of some of these genes in neural progenitor cells leads to larger clone size and potentially, a higher number of neurons to be generated. In parallel, expression of the same genes in mouse testicular progenitor cells gave rise to much more enhanced 3D clonal formation ability, indicating a clear upgradation of the mouse reproductive system.

In summary, these findings support the hypothesis that there exist primate-specific “smart-and-sex” genes that could be the evolutionary driver for neuron and germ cell development in primates, with great therapeutic potential in treating neural and reproductive diseases.

Keywords: brain, testis, cortical neurogenesis, spermatogenesis, neural stem and progenitor cell, spermatogonial stem and progenitor cell, primate, evolution

CONTENTS

1. RESEARCH BACKGROUND AND SCIENTIFIC HYPOTHESIS

1.1. Brain developmental difference between primates and non-primate mammals

Primates exhibit more intelligence than other mammals, with humans at the top. Over millions of years, primate brains have evolved to become dramatically larger relative to primate body size (1-4). The surface area of the cerebral cortex in non-human primates and humans is much larger than that of mice, with an approximate ratio of 1:100:1000 (mouse: macaque monkey: human), while the cortical thickness of macaque monkeys and humans is similar, approximately twice that of mice. In addition to the overall increase in brain size, to further enhance cortical complexity, primates have evolved some specialized brain regions (1-4). The prefrontal cortex, for example, has expanded significantly in humans, allowing for more complex cognitive functions (1-4). These observed trends in brain development suggest that cognitive abilities have been a strong selective pressure throughout the evolution of primates. It's as if nature decided that "being smart" was the way to go, and primates had selected the right path.

The markedly larger brain size of primates is due to neocortex expansion, a hallmark of primate evolution (1,5-7). Although cortical neurogenesis is mostly conserved among mammals, there exist species-specific mechanisms of cortical neurogenesis in primates (8,9). One salient difference between primates and non-primate mammals is the timing of neurogenesis. Cerebral cortical development in primates extends over a longer duration compared with non-primate mammals, giving rise to prolonged proliferation of neural progenitor cells and the increased size and complexity of the primate cortex (Figure 1) (8,9). Another major difference between primates and non-primate mammals lies in the outer radial glial cells (oRGC), a major class of progenitor cells, which carry highly proliferative abilities and undergo considerable amplification during primate cortical neurogenesis (8-12). The highly expanded oRGC pool contributes to the increased cortical size by adding an additional layer in the primate cortex, the outer subventricular zone (OSVZ), which constitutes most of the proliferative region at later stages of corticogenesis and results in the latest-generated neuron and an increased proportion of glial cells in the primate cerebral cortex (Figure 1) (8,9).

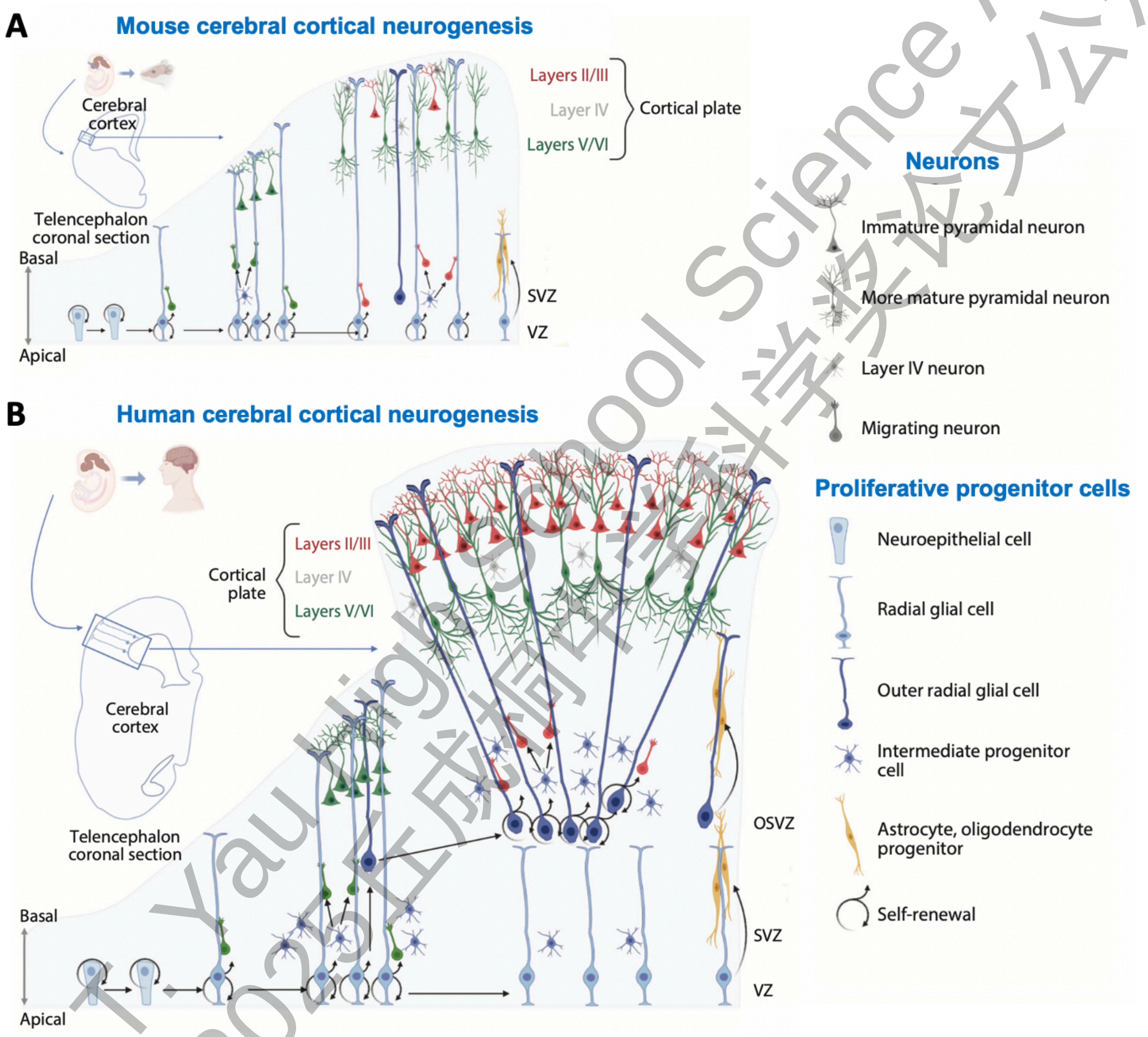

Figure 1. Comparison of cerebral cortical neurogenesis in mouse (A) and human (B). Human cortical neurogenesis involves a higher diversity of neural progenitors, which accounts for a higher number of cortical neurons. In primates, outer radial glial cells are amplified in the OSVZ and constitute an additional pool of progenitors, as well as a scaffold for neuronal migration. VZ: ventricular zone; SVZ: subventricular zone; OSVZ: outer subventricular zone. Picture is adapted from Libé-Philippot B., Vanderhaeghen P. *Annual Review of Genetics* (2021) (8).

Then, are there any primate-specific “smart genes” that could play a crucial role in primate brain evolution? Considerable efforts have been made to identify such genes, yet so far this remains challenging (8,9). While a handful of candidate genes unique to primates have been characterized functionally for their roles in primate cortical expansion (8,9,13-20), the search for “smart genes” in primates is still in its infancy. How can we uncover these primate-specific “smart genes”, if any?

1.2. Brain and testis are most similar among human organs

When studying brain-related genes, one cannot miss brain-testis similarities. Despite their functional and morphological differences, it has become increasingly recognized that the brain and testis, among all the organs of the human body, strikingly exhibit the most similar gene expression pattern (21,22). Not only at the transcriptome level, but at the protein level human brain and testis also shared the most similar proteomes among 33 representative organs in the human body (23). Specifically, among the 14,315 proteins that make up the human brain and the 15,687 proteins that constitute the testis, 13,442 proteins are shared by both (23). These data indicate that the brain and testis are, in fact, the most similar organs in the human body. Further, in a recent study scientists found a positive correlation between male intelligence and sperm quality (24). Altogether, multiple lines of evidence suggest that there might be a certain “mysterious connection” between human brain and testis.

1.3. Scientific hypothesis—“smart-and-sex” genes in primates

Why do the brain and testis, two seemingly unrelated organs, exhibit a high degree of similarity? A comparison of neural stem/progenitor cells (NSPC) and spermatogonial stem/progenitor cells (SSPC) in primates versus non-primate mammals may provide a clue. SSPCs, the foundation of spermatogenesis, are essential for male fertility via two key functions: self-

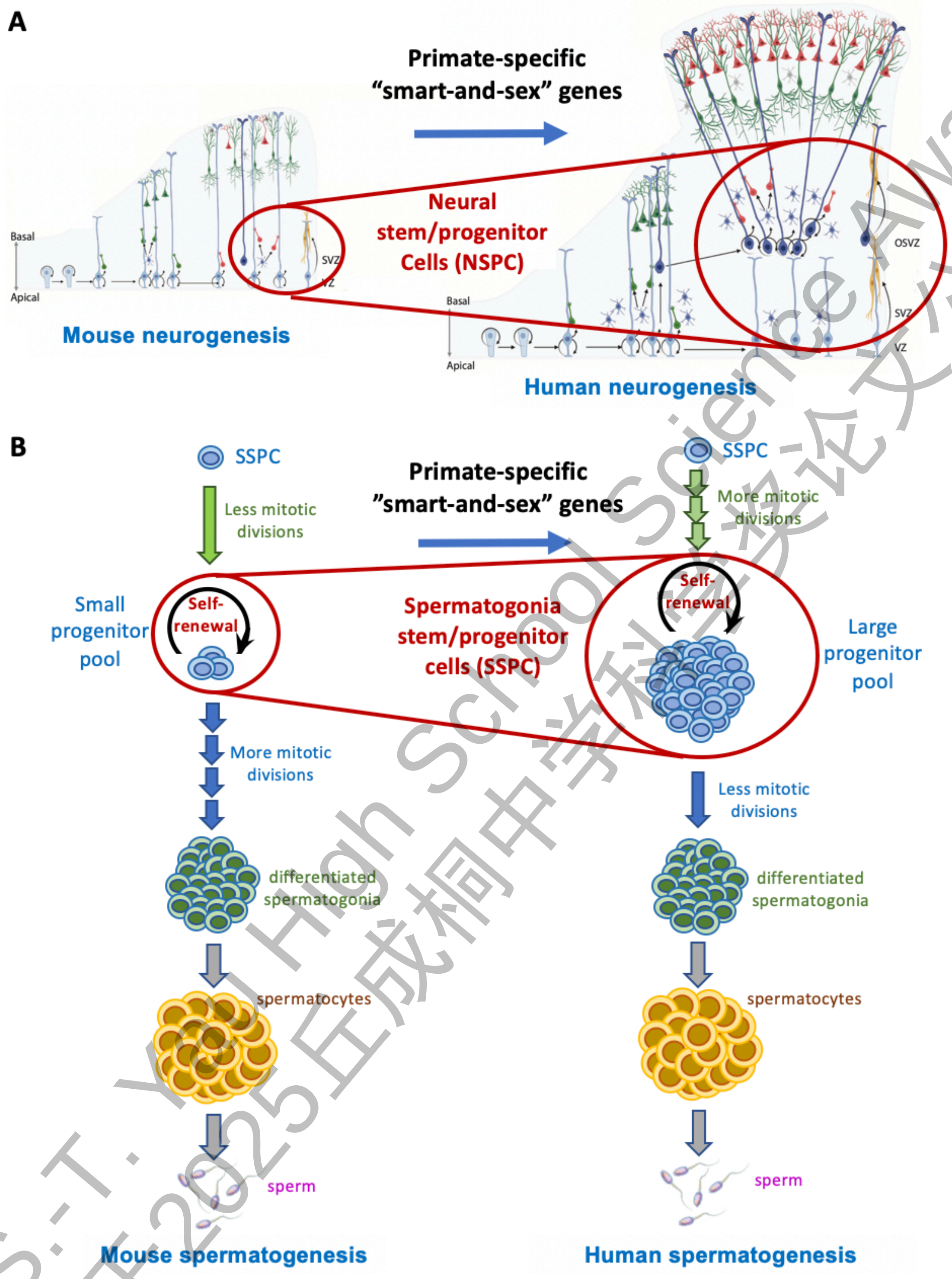

Figure 2. The “smart-and-sex gene” hypothesis. I hypothesize that there exists a group of primate-specific “smart-and-sex” genes that play important roles in the enhanced proliferation of both neural stem/progenitor cells (NSPCs) and spermatogonia stem/progenitor cells (SSPCs) (denoted by red circles). Pictures are adapted from Libé-Philippot B., Vanderhaeghen P. *Annual Review of Genetics* (2021) and Fayomi, A.P. and Orwig, K.E.et al. *Stem Cell Research* (2018) (8,9).

renewal to maintain the SSPC pool and differentiation to maintain the stable sperm production

(25-28). Non-primate mammals contain a small number of SSPCs that undergo numerous rounds of mitotic divisions for sperm production (29). Contrarily, primates maintain a large pool of SSPC with an enhanced self-renewal ability which constitutes an increased proportion of germ cells in testis (30-33), mirroring primate neural progenitor cells' proliferation pattern. This larger pool of SSPC in primates represents a mechanistic "upgradation" to protect the male germ cells from the risk of mutations in longer-lived primates (25-28).

The observation of parallel increase of progenitor cell pools of brain and testis in primates versus non-primate mammals prompts me to hypothesize that the "mysterious connection" between human brain and testis may come from some "smart-and-sex" genes in primates that potentially govern the upgradation of the progenitor systems in both brain and testis and contribute to the development of primates' advanced cognitive and reproductive traits. In fact, the "smart-and-sex″ genes, if any, may become the answer to my quest for "smart genes".

2. MATERIALS AND METHODS

Identification of primate-specific genes

Homology data for human–mouse (*Homo sapiens–Mus musculus*) and human–wild pig (*Homo sapiens–Sus scrofa*) were downloaded from Ensembl 112 (released May 2024) via biomaRt (2.48.3). Human gene basic information (ensembl_gene_id and external_gene_name) was retrieved, and homologous Ensembl IDs and gene names for *M. musculus* and *S. scrofa* were extracted. Genes present in the human genome but absent in *M. musculus* were selected as human-specific genes, and those with recorded homologs in *S. scrofa* were further excluded. After this filtering, a total of 1,680 prospective primate-specific genes were retained for subsequent analyses.

Gene expression pattern analysis of different organs and different developmental stages

To investigate organ- and developmental stage-specific expression of primate-specific genes, I integrated multiple transcriptomic datasets. Adult tissue gene expression matrices and sample information were obtained from GTEx, and human fetal gene expression matrices were retrieved from E-MTAB-6814, including forebrain/cerebral cortex, cerebellum, heart, kidney, ovary, testis, and liver.

The processed expression matrices were used for unsupervised hierarchical clustering to identify stage-specific expression patterns in human brain. Based on the clustering results, genes were classified into three developmental stage-specific groups: 0-1year-specific (Group A), postnatal-specific (Group B), and prenatal-specific (Group C). Subsequently, hierarchical clustering was applied to standardized expression matrices using the R package pheatmap (v1.0.12), and heatmaps were generated to visualize gene expression patterns across different organs and developmental stages.

Molecular cloning and "smart-and-sex" gene overexpression plasmid construction

The fragments of 12 selected "smart-and-sex" genes (CT47B1, CTAG2, FMA9A, FTHL17, GAGE1, GAGE2A, MAGEA8, MAGEC1, PAGE5, TFDP3, VCX3A, and SAGE1) were synthesized by Sangon Biotech and ligated into the Flag-tagged plasmid pCDH-CMV-MCS-EF1-copGFP through EcoRI and NotI. These pCDH-CMV-SnS-EF1-copGFP plasmids were then transfected into HEK293 cells for virus production (SnS: smart-and-sex gene). The fragments of these "smart-and-sex" genes were also ligated into the PB-TET3G-PURO vector through EcoRI and MluI. These PB-TET3G-SnS-PURO plasmids were then transfected into human embryonic stem cells H9. Briefly, the backbone PB-TET3G-PURO and pCDH-CMV-MCS-EF1-copGFP vectors were digested with restriction endonucleases at 37°C in a water bath for 2 hours. Then, the vectors were extracted by using agarose gel DNA recovery kit (Tiangen, #DP209). After ligation with gene fragments at 16°C overnight, the mixture was transformed into *Escherichia coli* DH5α competent cells. Positive clones were selected and then validated by DNA sequencing.

Maintenance of human embryonic stem cells H9 in mTeSR™

Sterile technique was used to prepare complete mTeSR™ Plus medium (Basal Medium + 5× Supplement). The following is an example for preparing 500 mL of complete medium. mTeSR™ Plus 5 × Supplement was thawed at room temperature (15 - 25°C) or overnight at 2 - 8°C. 100 mL of mTeSR™1 5 × Supplement was added to 400 mL of mTeSR™ Plus Basal Medium and mixed thoroughly. A successful culture of human ES cells in mTeSR™ Plus requires the use of a suitable matrix to allow the attachment of cell aggregates. ESC-H9 cells were cultured in mTeSR™ Plus using Corning Matrigel (catalog number 354277, lot number 12924003). 250 μL Matrigel was added to 50 mL DMEM-F12 medium and mixed thoroughly. 2 mL diluted Matrigel solution was immediately added to 6-well plates, and incubated at room temperature for at least 1 hour before use. Human ESC-H9 colonies were detached using ReLeSR™. Cells were harvested by pipetting up and down with a 1 mL pipettor to ensure a detached-cell solution, and the cells were then transferred to a 15 mL conical tube. An additional 2-4 mL of medium (mTeSR™ Plus) was added to the tube containing the cells. Cells were centrifuged at 300 × g for 5 minutes. Cells were resuspended in the appropriate medium for later experiments. The cell aggregate mixtures were plated at the desired density onto coated wells containing mTeSR™ Plus. The plates were incubated in a 5% CO_2, 37°C incubator. Daily medium change was performed using mTeSR™ Plus, and the cultures were visually assessed to monitor growth until the next passaging time or further experiments.

Establishment of Tet-On 3G “smart-and-sex” gene inducible ESC-H9 cell lines

Human ESC-H9 cells were seeded in a 6-well plate at a density sufficient to reach near confluence at 48 hr after transfection. Three plasmids (1 µg PB-TRE3G-SnS-PURO + 1 µg PB-EF1a-TET3G + 1 µg EF-1a intron A) were simultaneously transfected into human ESC-H9 cells using Lipofectamine^{TM} stem cell transfection reagent (STEM00015). On the day of transfection, the following steps were performed (Table 1).

Table 1. Transfection steps.

Timeline		Step	Procedure details
Day 0	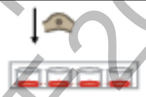	Seed cells to be 30–60% confluent for transfection	Adherent stem cells: 1 × 10^5 cells per well in a 6-well plate
Day 1		Add Lipofectamine™ Stem Reagent in Opti-MEM™ I Medium	Opti-MEM™ I Medium 50 µL
			Lipofectamine™ Stem Reagent 12 µL
Day 1		Add plasmids in Opti-MEM™ I Medium	Opti-MEM™ I Medium 50 µL

			3 plasmids: PB-TRE3G-SnS-PURO 1 µg PB-EF1a-TET3G 1 µg EF-1a intron A 1 µg
		Add diluted plasmids to diluted Lipofectamine™ Stem Reagent (1:1 ratio)	Diluted plasmids volume
			Diluted Lipofectamine™ Stem Reagent volume
		Incubate	Incubation for 10 minutes at room temperature.
		Add DNA-lipid complex to cells	Adding Gently.
Day 4	Puromycin 	Puromycin selection	Incubate and monitor transfected stem cells at 37°C for 4 days. The concentration of puromycin was 0.2 ng/mL.

Quantitative reverse-transcription polymerase chain reaction (qRT-PCR)

The qRT-qPCR assay consists of three steps: reverse transcription, qPCR, and data analysis. RNA extraction was performed following the manufacturer's instruction (Takara #9109). RNAs prepared by the RNeasy Mini kit were treated with DNase (Qiagen #79254, USA). Reverse transcription was performed using Hiscript III Reverse Transcriptase (Vazyme). Quantitative PCR was performed using AceQ qPCR SYBR Green Master Mix (Vazyme) on a QuantStudio™ Real-Time PCR instrument. PCR primers were designed using the NCBI PrimerBLAST tool (Table 2).

Table 2. qRT-PCR primers.

	Forward primer (5'-3')	Reverse primer (5'-3')
MAGEC1	CAGCGGAGGGAGGAGACTTA	GGCATATCCTTGTCCCCCAT
VCX3A	AGAGGGATGATTGACGTCTTCG	CCAGCCAATGGTAGCCCTAAAA
FAM9A	GGGGCCACGAAAGAAGGT	CGGACTGGATCCTTTCCTGTG

MAGEA8	AGCACTGAAGAAGACCTGCCTGT	ATCCATAAGCCCTGGTGCCT
CT47B1	CAGATGAGAAACCCCCAGA	GAGATTTAGTGACTTCCTCGG
FTHL17	TCGGACGACAAAATGGAGCA	CAGGCTCTGGTTGACGTTCT
GAGE2A	GGCCTAGACCAAGACGCTAC	TTCAGGCTTCGGCCCTTG
TFDP3	CTTTTGGGCTAGAGTCCGGG	CTGAGATCCACCGGAGCTTG
PAGE5	CCTGCTGTTCAAGGGACTGA	ACCTATAGTTGCCCTTCACCT
GAGE1	TGCAGGTCAAGGGCCGAAG	TCTTCTTTTAACACTGTGATTGCCC
CTAG2	GCCTGCTTGAGTTGCACA	CGGACACGGTGAAGTCCT
SAGE1	ATCCTTACGCCACCATCACAT	GTTCCTGCTCCTGCCACAT

Western Blot

Lysates from cell cultures were prepared following the manufacturer's instruction. Briefly, cells were washed with PBS and lysed with 500 µL lysis buffer (50 mM Tris-HCl, 150 mM NaCl, 1 mM EDTA, 0.05% Triton-X100, 0.1% Sodium deoxycholate, 5% Glycerol, and 1% protease cocktail (MCE #HY-K0012). Cell lysates were centrifuged, and the supernatants were transferred to a new tube. An equal amount of proteins from each sample was loaded into gels (GenScript M00657). After performing electrophoresis, proteins are then transferred onto PVDF membranes (Millipore # IPVH00010). The blots were incubated in blocking buffer (5% fat-free milk in TBS buffer) at room temperature for 1 h. The PVDF membranes with proteins were incubated with specific antibodies (Table 3) at 4°C overnight with rocking. Blots were then washed and incubated in the HRP-labeled secondary antibodies at RT for 1 h. After washing, blots were developed using the ECL Prime substrate and imaged using the GE Amersham Imager 600 system.

Table 3. antibody information

Name	Company	Cat number	Dilution
MAGEC1	Santa Cruz	sc-53868	1:50
VCX3A	Novus Biologicals	H00051481-B01P	1:100

FAM9A	Merke	HPA056076	1:200- 1:500
MAGEA8	proteintech	15045-1-AP	1:100
CT47B1	Biorbyt	orb2307013	1:100
FTHL17	Biorbyt	orb2306795	1:100
GAGE2A	Biorbyt	orb2307281	1:100
TFDP3	Biorbyt	orb400660	1:200
PAGE5	Invitrogen	PA5-50470	1:100
GAGE1	Proteintech	12795-1-AP	1:100
CTAG2	Invitrogen	PA5-64462	1:100
ACTL8	ThermoFisher	PA5-21788	1:50
SAGE1	Novus Biologicals	NBP-84355	1:200
FLAG	Sigma	F1804	1:1000
PAX6	CST	60433S	1:500
MAP2	Abcam	Ab5392	1:20000

Immunofluorescence staining

Human testicular tissues were fixed in 4% PFA and embedded in paraffin. Briefly, 5-μm-thick paraffin sections were mounted on polylysine-coated slides, baked in the oven at 60°C, dewaxed with xylene, and rehydrated through a graded series of ethanol solutions. After rehydration, slides were covered with the appropriate antigen repair buffer in a microwave for 15 min at 20% power, and then blocked. Primary antibody was diluted and applied to the specimen, which was then incubated with fluorochrome-conjugated secondary antibody (Table 3). DAPI (Thermo Fisher #D1306: 1:1000) was applied for DNA staining and mounted. Slides were examined using laser scanning confocal microscopy (Leica, SP8 STED 3X).

Mouse SSPC cells, human ESC-H9 cells, or ESC-H9-derived neuronal cells were fixed with 4% PFA, permeated with 0.2% Triton X-100-PBS, and blocked with blocking buffer. Primary antibody was diluted and applied to the specimen, which was then incubated with fluorochrome-conjugated secondary antibody (Table 3). Slides were stained with DAPI (Thermo Fisher #D1306) and mounted for imaging.

Neural differentiation from human ESC-H9

For neural differentiation, on day 0 cells were dissociated using Stem-Pro Accutase (Invitrogen A11105) and plated on Matrigel (BD) coated-coverslips/dishes at low confluency (5,000 cells/cm^2) in mTeSR™ Plus medium supplemented with ROCK inhibitor (Y-27632; 10 μM Calbiochem, 688000). On day 1, the medium was changed to mTeSR^{TM} Plus medium, On day 2, the medium was changed to DDM, supplemented with B27 minus VA (10 ml B27 minus VA per 500 ml DDM to increase the survival) and Noggin (100 ng/ml), and the medium was replenished every 2 days. After 16 days, the medium was changed to DDM, supplemented with B27, and changed every 2 days. After 24 days, the progenitors were manually dissociated, and cells were resuspended in DDM supplemented with B27 and ROCK inhibitor (10 μM) and plated onto Matrigel. Five to seven days after dissociation, half of the medium was replenished with Neurobasal supplemented with B27 (10 ml B27 per 500 ml DDM) and 2 mM glutamine, and changed again every 5–7 days. ESC-H9-derived neuronal cultures were ready for IF staining by anti-PAX6 and anti-MAP2 antibodies.

Isolation of SSPC cells from mouse testes

Mouse testis samples, washed three times with PBS, were minced with sterilized scissors and subjected to a standard two-step digestion procedure as described previously (34,35). Briefly, testicular tissues were digested with collagenase type IV (Sigma Aldrich #C5138-500MG) for 5 min at 37 °C with gentle agitation (180 rpm), then shaken vigorously and incubated for another 3 min. The tubules were sedimented by centrifugation at 90 × g for 3 min and washed with PBS before digestion with 4.5 mL 0.25% trypsin Invitrogen #15050065) and 4 kU DNase I (Sigma Aldrich #D4527-500ku). The suspension was triturated vigorously three to five times and incubated at 37 °C for 5 min. The digestion was stopped by adding 10% FBS (Gibco

#A5669701). Testicular cells were obtained by filtering through 40-μm nylon cell strainers (Corning #352340) under sterile conditions. The filtrate was pelleted by centrifugation at 500 × g for 5 min, and washed twice with 1 × PBS. Cell number was measured using a hemocytometer, resuspended in complete medium. Gelatin is used for somatic cell attachment in 10 cm dish overnight. The somatic cells were attached, the mouse SSPCs in medium were transferred to a fresh tube and harvested for further experiments.

Lentivirus preparation

HEK293T cells from American Type Culture Collection (ATCC) were cultured in Dulbecco's modified Eagle's medium (DMEM) (Gibco 11965092) supplemented with 10% fetal bovine serum (Gibco). 15 h before transfection, 8×10^6 cells were plated in a 15-cm dish for a confluency of 70% by the next day. The "smart-and-sex" gene expression plasmid (16 μg) and packaging vectors (p-VSVG, 8 μg; DR8.9, 12 μg) were mixed with Lipofectamine 3000 (Life Technologies), transiently transfected into HEK293T cells. After at least a 48-h incubation period, the virus-containing supernatant was harvested and concentrated. Finally, the virus was resuspended in 1 mL SPG medium.

Lentivirus infection

The lentiviral solution was rapidly thawed at room temperature. 1 mL lentivirus, 9 mL SSPC medium, and 10 μg mL^{-1} polybrene were mixed to prepare the virus solution. 1×10^6 mouse SSPC cells were resuspended with the virus solution and incubated for 24-36 h. Then, the media was replaced with 10 mL fresh SSPC medium. The infection efficiency was validated on Day 5 by GFP fluorescence.

Flow cytometry

The infected mouse SSPC cells were harvested to prepare a single-cell suspension. SSPCs were re-suspended at a concentration of 2-5×10^6/mL, and filtered to prevent clogging. A sorting speed of approximately 18,000-20,000 events per second was maintained at the optimal pressure. The collection medium was supplemented with 10% serum. Mouse SSPCs expressing the GFP tag were collected in FACS tubes. The sorted cells carrying SnS-GFP or EV-GFP were used for IF staining and 3D colony formation assays.

3D spheroid formation assay

Matrigel matrix (Corning # 356321) was thawed overnight by submerging the vial in 4°C before use. Mouse SSPCs were harvested to make a single-cell suspension, pelleted, and gently resuspended with Matrigel matrix using pre-chilled tips. A mixture of 50 µL Matrigel matrix and 1,000 mouse SSPC cells was added to each well (24-well plate, PerkinElmer), incubated at 37°C for 10 min. 1 mL of mouse SSPC medium was added to each well. The cultures were maintained at 37°C in an incubator with 7% CO_2 and 5% O_2 for 35 days, and half of the medium was changed every 3 days. The colonies were fixed in 4% PFA and stained with 0.5% Crystal Violet, or visualized by GFP under a fluorescent microscope. The images of Crystal Violet staining-3D cultures were collected by a ZEISS Zoom V16 microscope. The number of colonies was calculated and analyzed by the ImageJ software.

3. RESULTS

3.1. Search for primate-specific “smart-and-sex” genes

If primate “smart-and-sex” genes do exist, they are likely primate-specific and emerged after the split between rodents and primates during evolution (here only protein-coding genes are referred to) (Figure 3A). To search for such genes, I first set out to obtain the list of primate-specific genes (PSGs), which can be generated by subtracting the aggregated non-primate mammalian genes from the aggregated primate genes. To simplify the process, I used the human gene-set as an approximation of the aggregated primate genes, and the sum aggregate of mouse and pig genes as an approximation of the aggregated non-primate mammalian genes (Figure 3B). All the gene information was retrieved from the Ensembl database (http://www.ensembl.org), and a total of 1,680 potential PSGs were identified (Figure 3B).

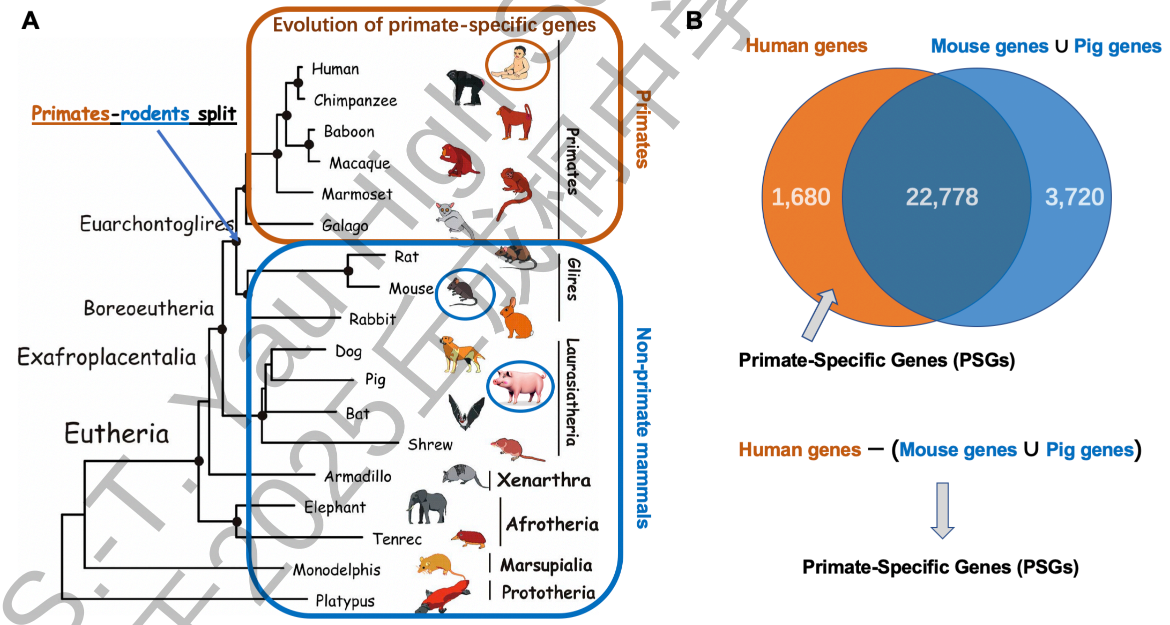

Figure 3. Identification of primate-specific genes (PSGs) by subtracting homologs of mouse and pig genes from the human gene set. (A) Phylogenetic tree of mammals. Orange and blue boxes denote primates and non-primate mammals, respectively. The position of the primate-rodent split is shown. **(B)** Venn diagram showing the overlapped human gene set and the sum aggregate of the mouse and pig genes. The PSG list is generated by the subtraction of the sum aggregate of the mouse and pig genes from the human gene set.

These PSGs may represent unique genetic codes that contribute to primate-specific traits in physiological, developmental, and cognitive functions.

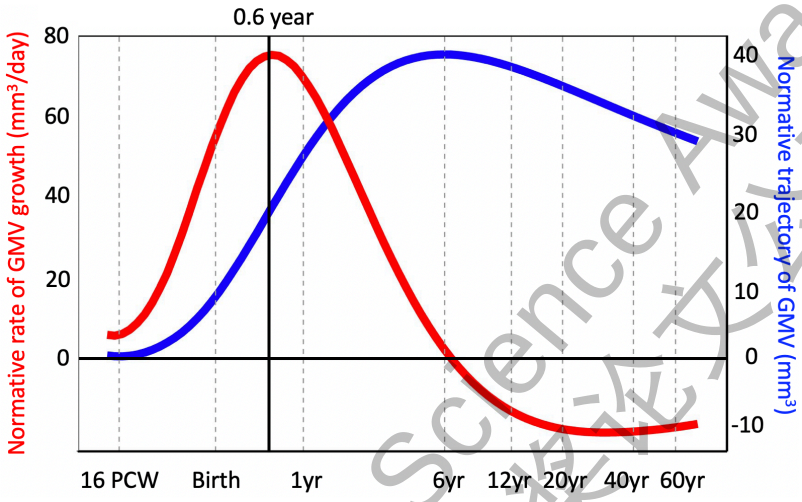

Figure 4. Normative grey matter volume (GMV) (blue line) and rate of GMV change (red line) across the human lifespan. Data are from Bethlehem R.A.I., et al. *Nature* (2022) (36).

In a previous study of brain charts across the human lifespan, it was demonstrated that grey matter volume (GMV) exhibits the fastest growth rate during the 0-1 year infant stage, which is considered a critical brain developmental window, corresponding to a large generation of neuronal synapses and initial construction of neural networks (Figure 4) (36). To explore the role of primate-specific genes in human early brain development, I compiled and analyzed the publicly available transcriptomic expression profiles of the human brain from 4 weeks post-conception (WPC) to

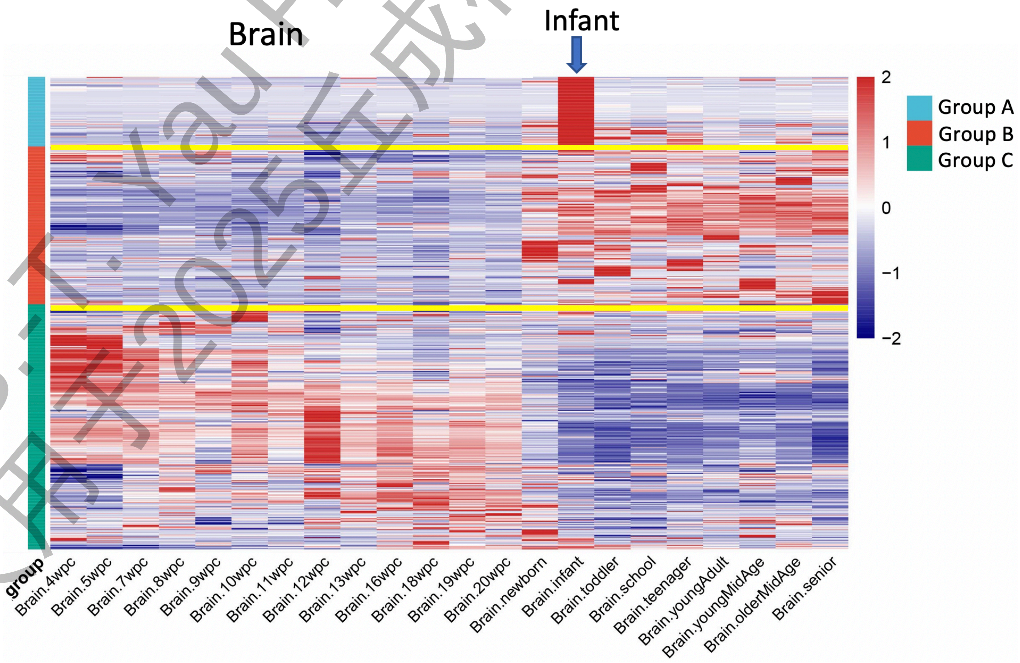

Figure 5. Primate-specific gene expression analysis in human brain from 4 weeks post-conception (WPC) to the age of 55 years.

the age of 55 years, including the 0-1 infant stage (37), to explore the role of PSGs in human early brain development. Notably, unsupervised hierarchical clustering bioinformatics analysis revealed that a group of PSGs exhibits a highly restricted expression only in the infant stage (Group A), while two other groups show expression postnatally (Group B) and prenatally (Group C), respectively (Figure 5). The striking coincidence in the infant stage of the fastest grey matter volume growth rate and the highly restricted expression pattern of Group-A PSGs strongly suggests that Group-A PSGs could play important roles in human infant cortical neurogenesis (Figures 4 and 5) (36,37).

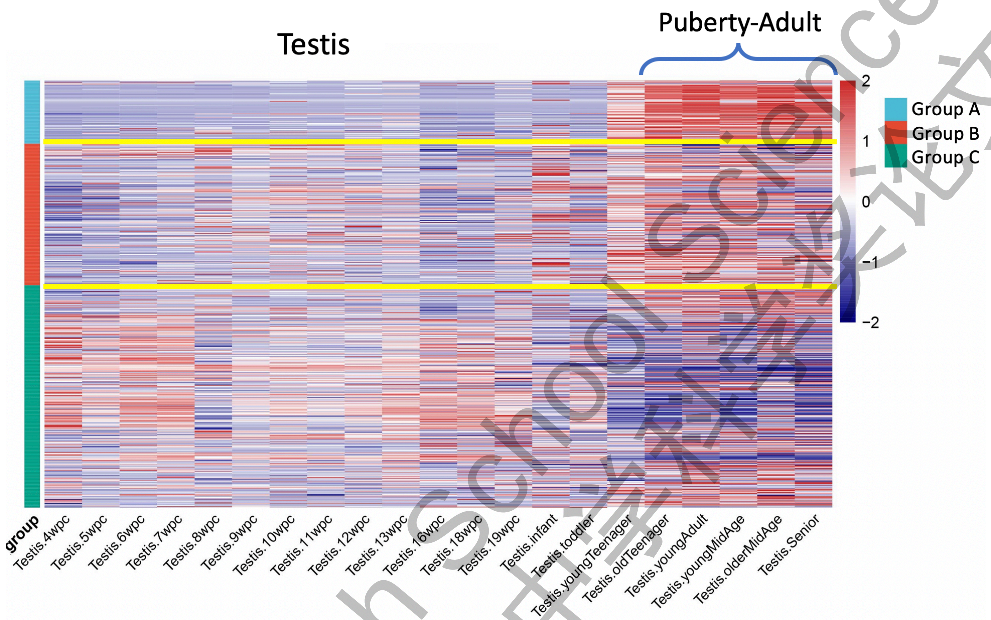

Figure 6. Primate-specific gene expression analysis in human testis from 4 weeks post-conception (WPC) to the age of 55 years.

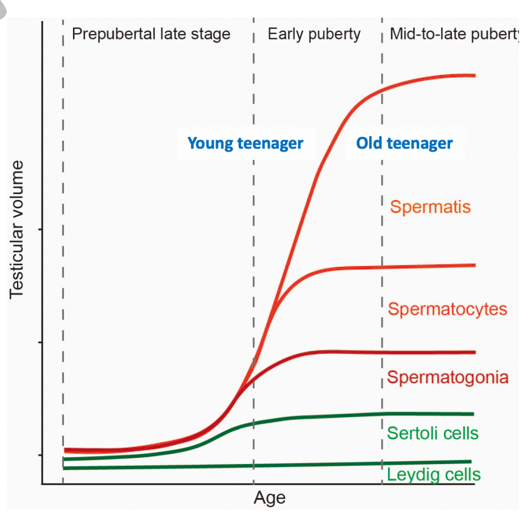

Figure 7. Schematic representation of pubertal testicular growth and distribution of testicular cell populations in humans. Data are from Kosjenniemi et al. *Curr Opin Endocrinol Diabetes Obes* (2017) (38).

To evaluate the role of PSGs in human testicular development, I compiled and analyzed the transcriptomic expression profiles of human testicular samples from 4 weeks post-conception to the age of 55 years (Figure 6). Markedly, the same group of PSGs (Group A) again exhibits the most unique expression pattern in testicular development. The overall expression levels of these Group-A genes are low before puberty (<13 years old), but collectively increase to a very high level upon entering the puberty age (around 14 years old), and are maintained at high levels through adulthood (Figure 6). A previous histological study shows that testicular growth quickly reaches a plateau during puberty, and this process is primarily driven by the rapid proliferation and establishment of a stable pool of human SSPC (Figure 7) (38). Interestingly, my analysis demonstrated that the upregulation of Group-A PSG expression corresponds to the period of rapid proliferation of SSPC, suggesting that Group-A PSGs might play key roles in the initiation and maintenance of spermatogenesis (Figures 6 and 7) (37,38).

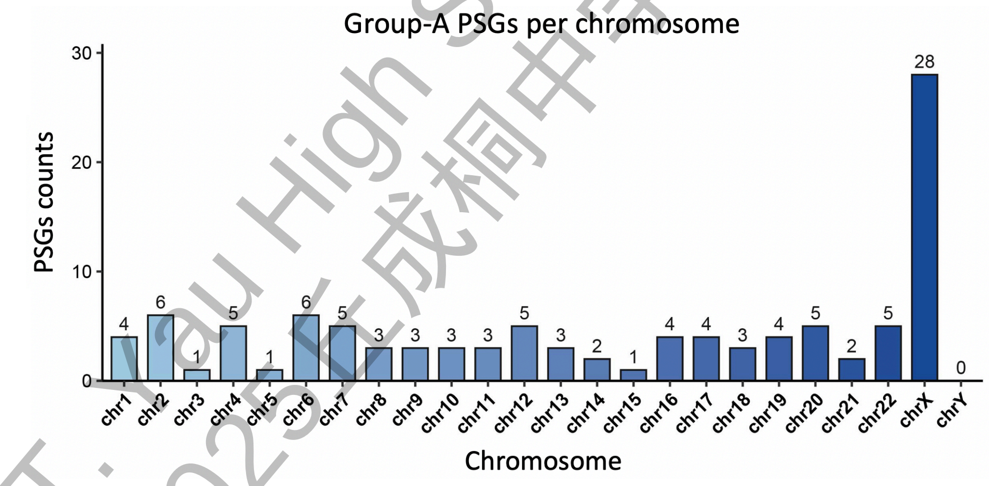

Figure 8. Chromosomal distribution of Group-A PSGs. About 26% of Group-A PSGs are clustered on the X chromosome.

It is noteworthy that the two distinct expression patterns of the same Group-A PSGs in the human brain versus testis match the proliferation patterns of the infant brain NSPC and the puberty-adult testicular SSPC, respectively, strongly suggesting that Group-A PSGs likely contain the sought-after “smart-and-sex” genes that could play key roles in both infant cortical neurogenesis and male spermatogenesis (Figures 4 and 5, 6 and 7). Intriguingly, chromosomal location analysis of group-A PSGs showed that these genes are not randomly distributed across the human genome, but exhibit a significant chromosomal bias—28 genes, approximately 26% of the Group-A genes, are located on the X chromosome (Figure 8). This highly skewed distribution pattern suggests that the X chromosome may be heavily involved in biological processes related to cortical neurogenesis and spermatogenesis in primates. Notably, most of these 28 prospective X-chromosomal “smart-and-sex” genes are uncharacterized, with few previous studies. Among them, I selected 12 genes whose antibodies are commercially available for further experimental exploration to test the “smart-and-sex gene” hypothesis (Figure 9).

Figure 9. The names and the X-chromosomal locations of 12 selected “smart-and-sex” genes.

3.2. Immunofluorescence staining confirms the expression of “smart-and-sex” genes in human testis

Next, I investigated the expression of 12 selected “smart-and-sex” genes at the protein level. Due to the sample limitation, I only performed an immunofluorescence (IF) staining characterization of a human testis sample obtained from Shanghai Jiao Tong University School of Medicine. The IF result clearly showed the expression of eight “smart-and-sex” genes (CTAG2, FAM9A, FTHL17, GAGE2A, MAGEA8, PAGE5, VCX5A, and SAGE1) in human testis (Figure 10). By contrast, the mouse testis did not show any detectable signals when using the same antibodies, confirming the human specificity of these “smart-and-sex” genes (data not shown). Therefore, the IF results confirmed the expression of eight of the 12 selected ‘Smart-and-Sex’ genes in human testis at the protein level.

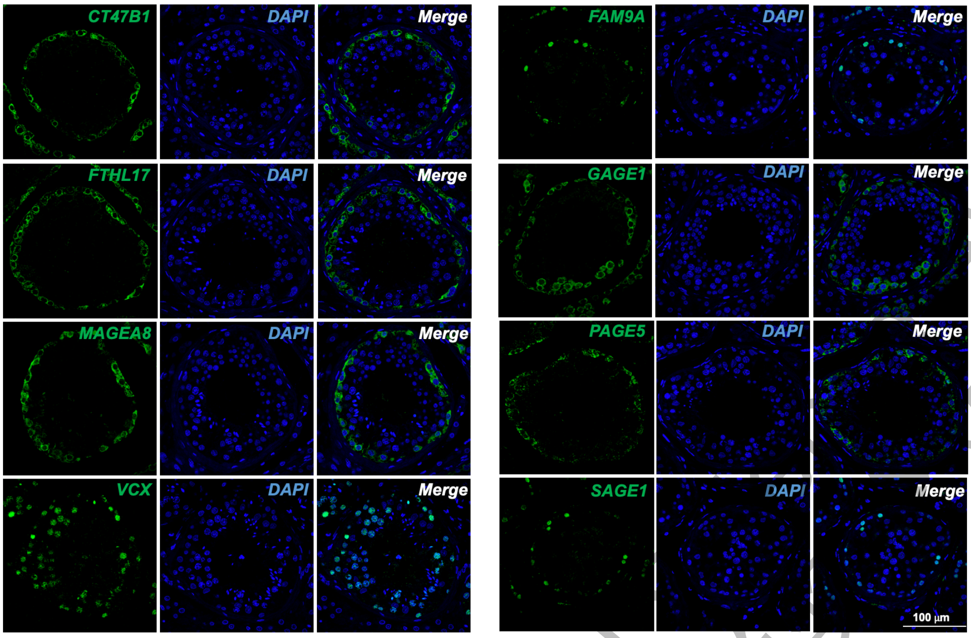

Figure 10. IF analysis shows the expression of eight selected "smart-and-sex" genes in human testis at the protein level.

3.3. Expression of "smart-and-sex" genes enhances the self-renewal of human neural progenitor cells

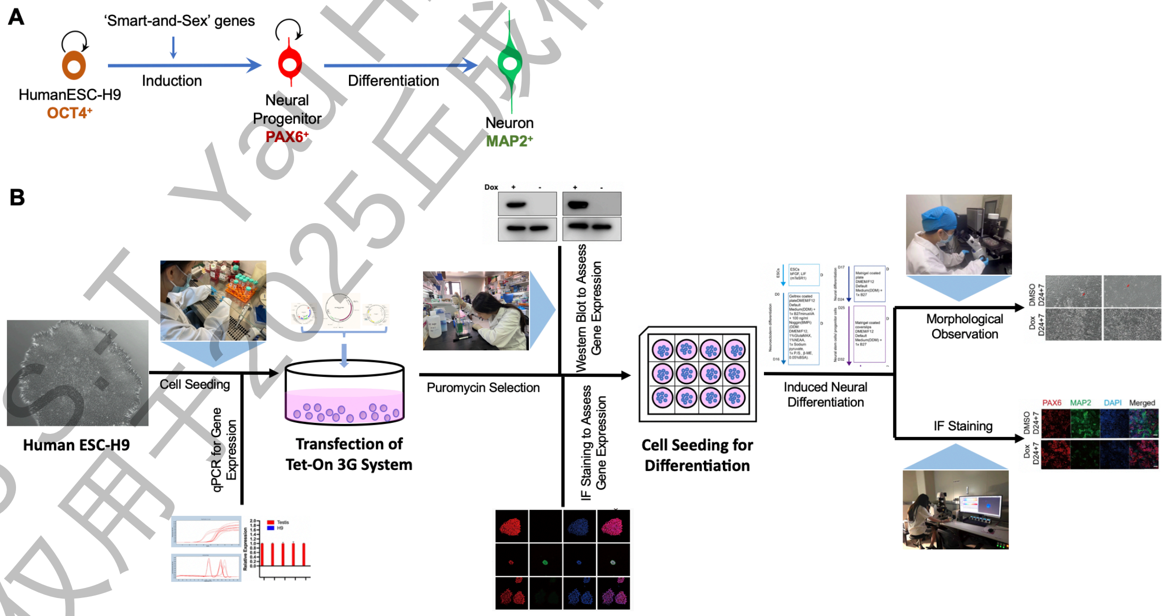

Figure 11. Examination of the function of selected "smart-and-sex" genes in human cortical neurogenesis. (A) Schematic illustration of the assay. **(B)** Flowchart of the experiments in Section 3.3.

3.3.1. Establishment of human embryonic stem cell lines with inducible expression of selected “smart-and-sex” genes

After the selection of 12 candidates of primate-specific “smart-and-sex” genes, I set out to characterize their functional significance in human corticogenesis. I employed a well-established *in vitro* model of cortical

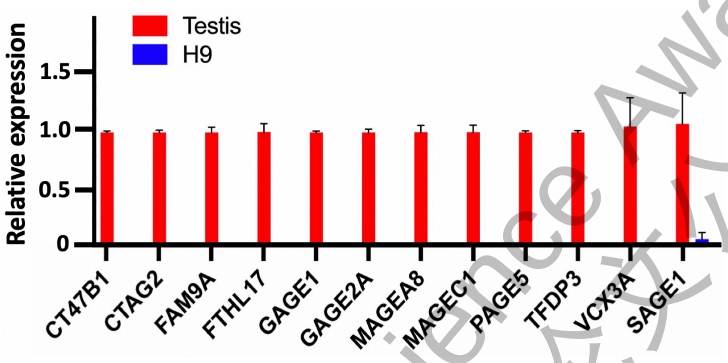

Figure 12. qPCR data show no detectable expression of selected “smart-and-sex” genes in ESC-H9 cells. qPCR data of human testicular cells were used as positive controls.

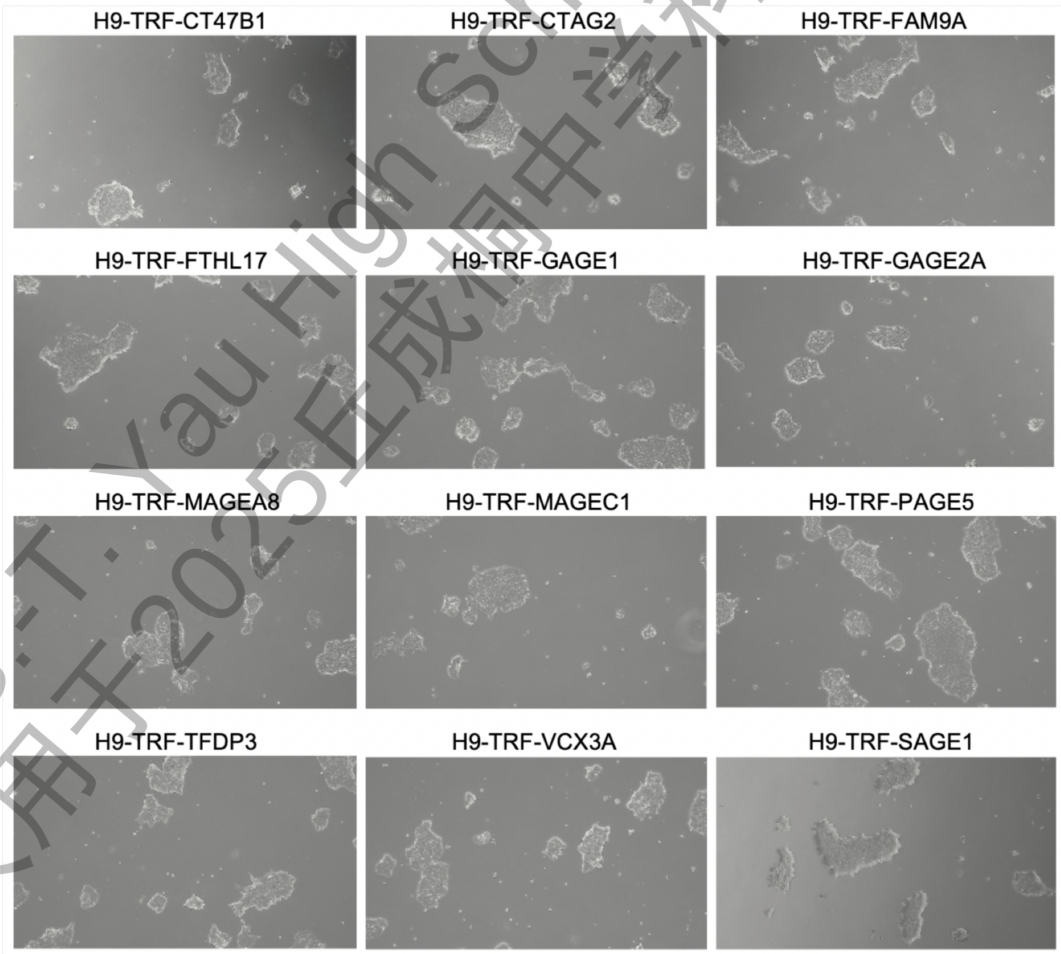

Figure 13. Establishment of human ESC-H9 cell lines with inducible expression of selected “smart-and-sex” genes. ESC-H9 clones were imaged by a bright-field microscope.

neurogenesis from human embryonic stem cells to investigate the impacts of these genes on cortical neurogenesis. In this model, the *in vivo* temporal dynamics of human cortical neurogenesis can be recapitulated in the *in vitro* procedures (15). Human H9 embryonic stem cells (ESC-H9) were cultured on Matrigel-coated dishes in the ES medium. Quantitative reverse-transcription polymerase chain reaction (qRT-PCR) analyses showed that, compared with human testis, human H9 embryonic stem cells (ESC-H9) exhibited no detectable expression of the 12 selected “smart-and-sex” genes (Figure 12), consistent with the fact that ESC-H9 is maintained in a pluripotent stem-cell state. Thus, I took a gain-of-function approach to evaluate the roles of “smart-and-sex” genes in cortical neurogenesis. I used an all-in-one, Tet-On-3G inducible PiggyBac system to achieve an inducible “smart-and-sex” gene expression in ESC-H9 (Figure 13, Table 1). The expression of “smart-and-sex” genes was examined at the protein level using Western blot and immunofluorescence staining assays to demonstrate that “smart-and-sex” gene expression was successfully induced by the addition of doxycycline (Dox) in ESC-H9 (Figures 14 and 15).

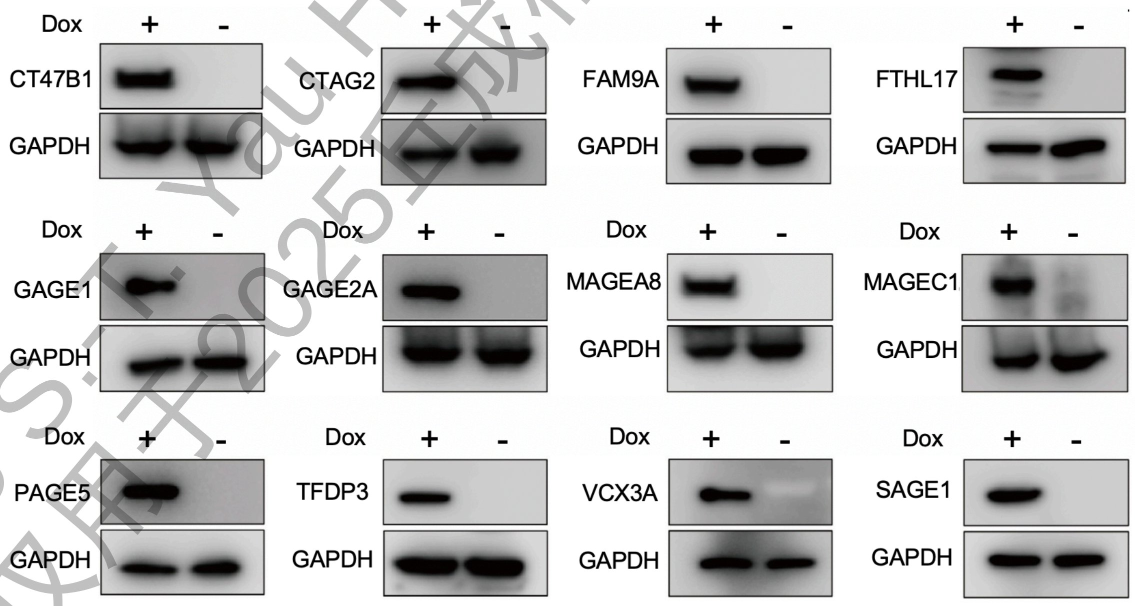

Figure 14. Western blot analysis shows the induced expression of “smart-and-sex” genes in ESC-H9 cells. Anti-Flag antibody was used to detect the expression of “smart-and-sex” genes.

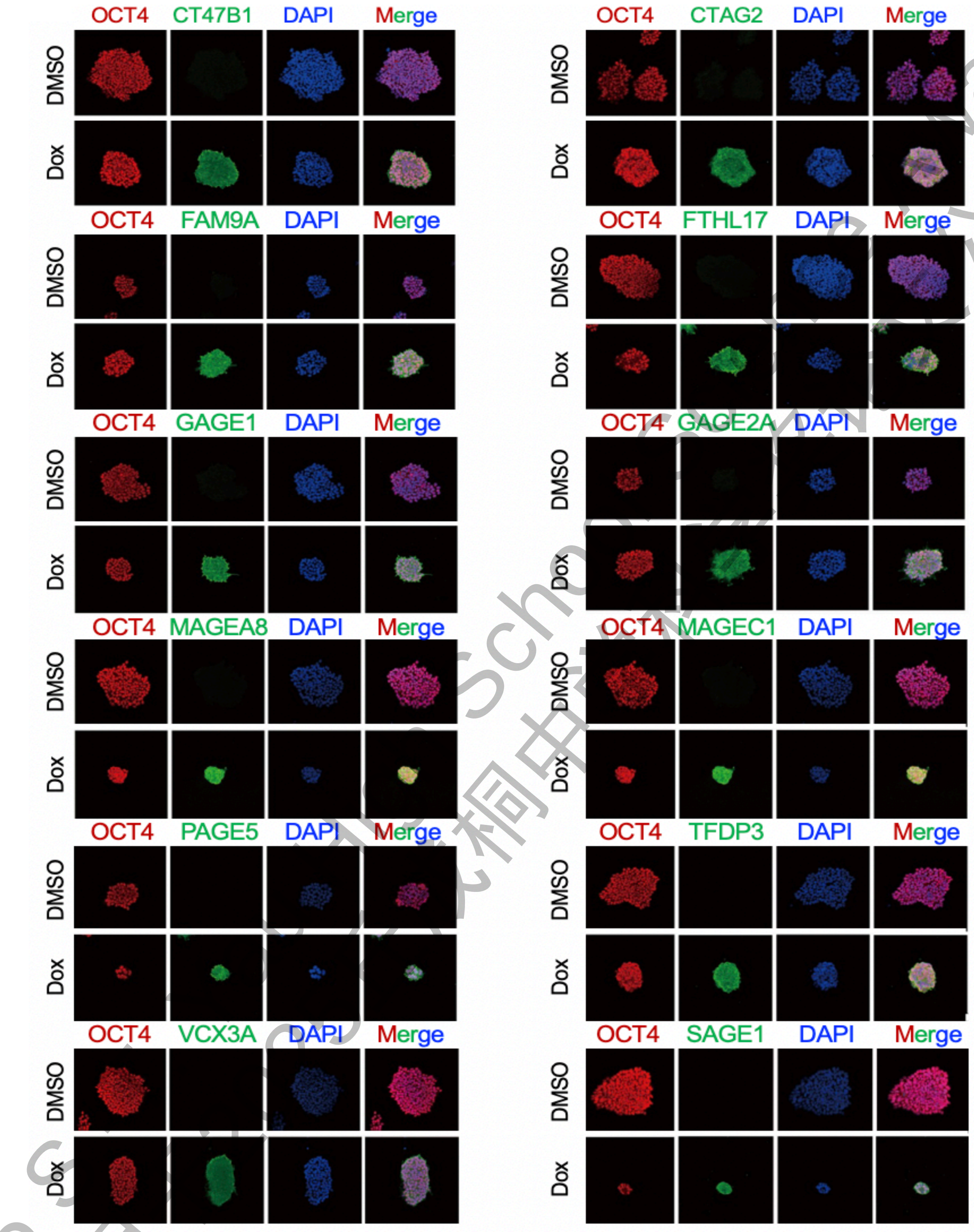

Figure 15. Immunofluorescence staining analysis shows the induced expression of Flag-tagged "smart-and-sex" genes in human ESC-H9 cells. "Smart-and-sex" genes were stained by anti-Flag antibody. OCT4 is a marker for ESCs. DAPI signals denote nuclear DNAs.

3.3.2. Expression of "smart-and-sex" genes enhances the self-renewal of PAX6$^+$ neural progenitor cells and inhibits the differentiation to MAP2$^+$ neurons

Next, I utilized the established Tet-On-3G inducible ESC-H9 cell lines to investigate the impacts of the selected "smart-and-sex" genes on clonal amplification and differentiation from cortical progenitors (Figure 11). To achieve a good effect, neural development and differentiation were induced from ESC-H9 cells at low confluency. After 24 days, images of the resulting neural progenitor cells were captured by a bright-field (BF) microscope. Remarkably, neural cultures derived from "smart-and-sex" gene-expressing ESC-H9 cells all showed higher cell densities than the controls (Figure 16). Additionally, "smart-and-sex" gene-expressing neural progenitor cells exhibited typical stem-cell morphology, while during the

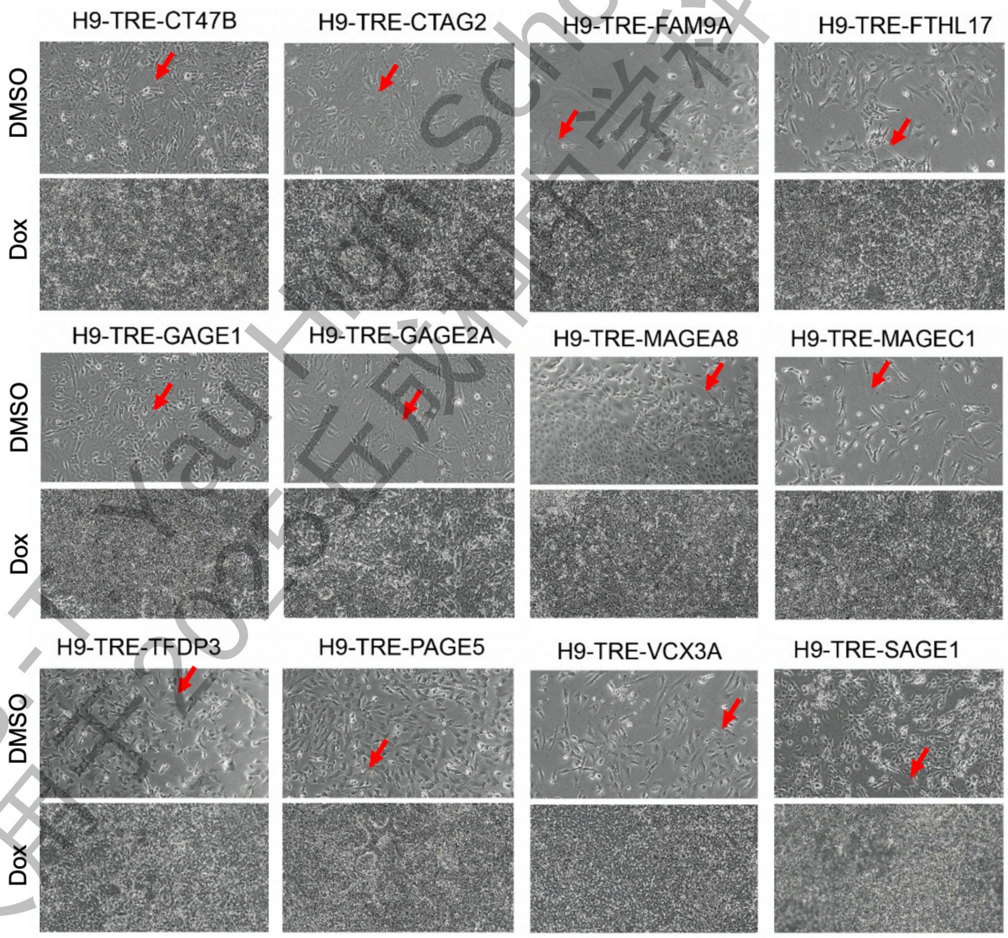

Figure 16. Bright-field microscopic images show that expression of the "smart-and-sex" genes increases the proliferation ability of neural progenitor cells and inhibits differentiation to neurons. Red arrows denote the axons of maturing neurons.

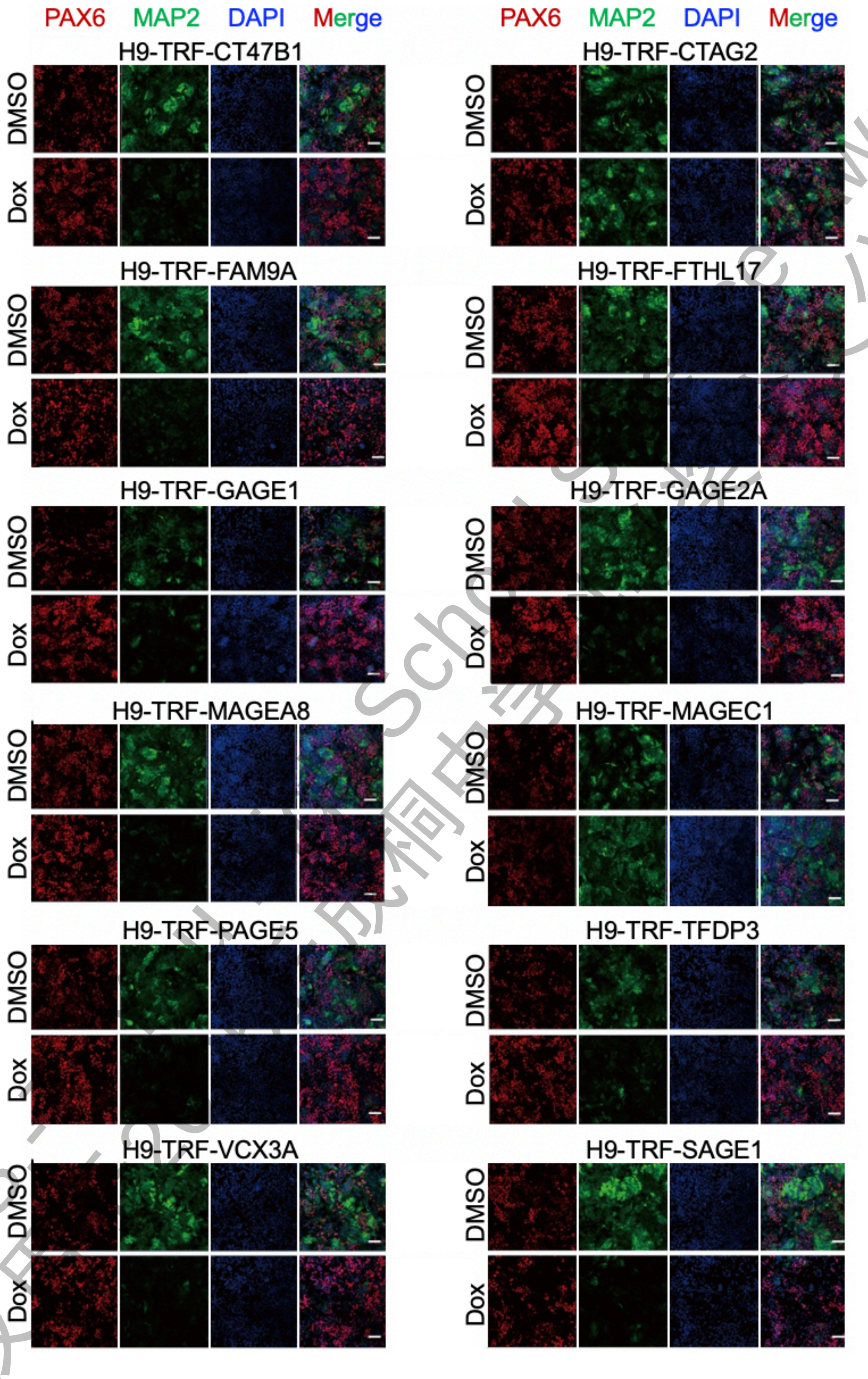

Figure 17. IF analysis shows that expression of the "smart-and-sex" genes increases the proliferation ability of neural progenitor cells and inhibits differentiation to neurons. PAX6 is a marker for neural progenitor cells, MAP2 is marker for neurons, and DAPI denotes nucleus DNAs.

same period, the control cells started to show signs of maturing neurons with long axons (Figure 16). These results indicate an increased capacity of "smart-and-sex" gene-expressing neural progenitor cells to expand clonally and maintain the neural progenitor state. Neural progenitor cells were cultured for an additional 7 days before they were IF stained by anti-PAX6 and anti-MAP2 antibodies (PAX6 is a marker for neural progenitors, and MAP2 is a marker for neurons). Consistent with the bright-field data, the IF images clearly showed that, except for CTAG2 and MAGEC1, expression of most selected "smart-and-sex" genes led to an expansion of PAX6$^+$ neural progenitors and inhibition of differentiation to MAP2$^+$ neurons (Figure 17).

Together, in alignment with the "smart-and-sex-gene" hypothesis, our data indicate that expression of primate-specific "smart-and-sex" genes during primate cortical development could enhance the self-renewal of neural progenitor cells, leading to a larger clone size, prolonged cortical neurogenesis with slower exhaustion of the progenitor pool, and ultimately, a higher number of neurons generated in primate brains (Figure 18).

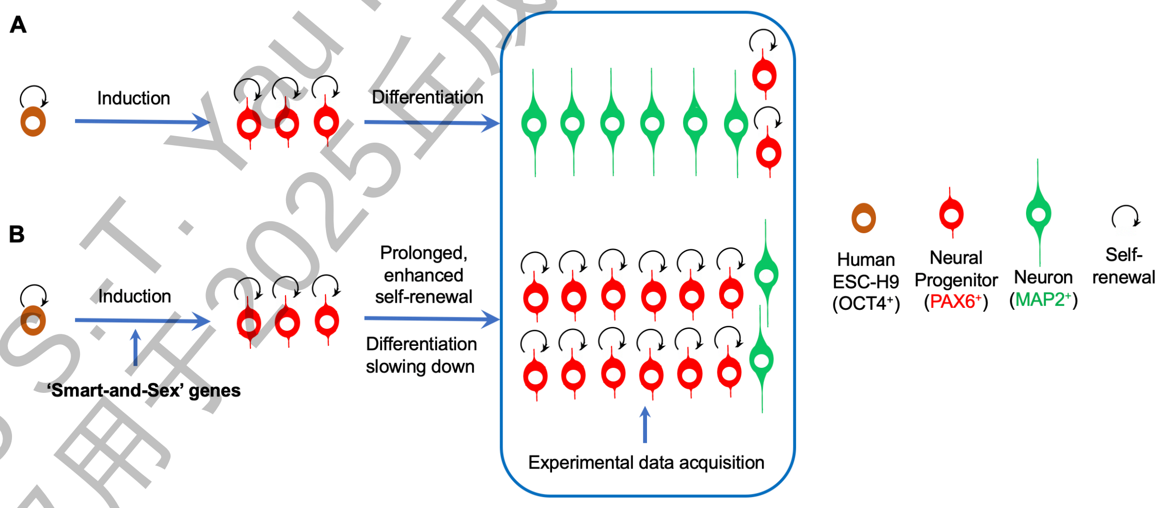

Figure 18. Summary of the results in Section 3.3. 'Smart-and-sex' gene expression leads to (1) enhanced self-renewal ability for neural progenitors, (2) a prolonged proliferation of neural progenitor cells, and (3) inhibition of the differentiation from PAX6$^+$ progenitors to MAP2$^+$ neurons.

3.4. Expression of human “smart-and-sex” genes enhances the clonal expansion of mouse spermatogonial stem and progenitor cells

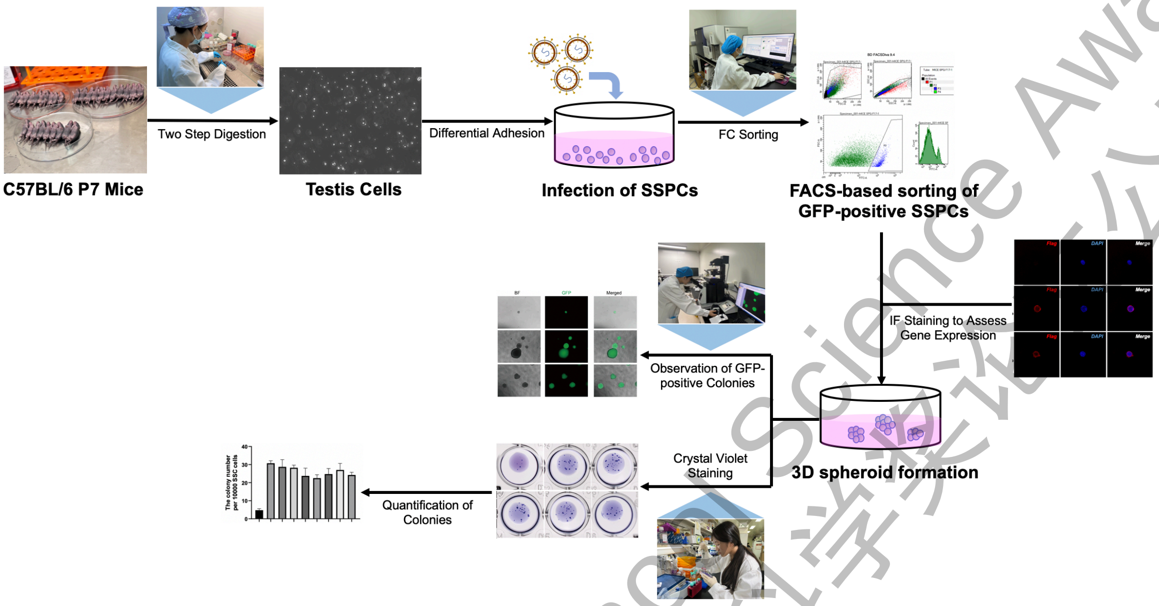

Figure 19. Flowchart of the experiments in Section 3.4.

Next, I set out to test the functional significance of the selected “smart-and-sex” genes in human testicular germ cell development. Given that the *in vitro* long-term culture of human spermatogonial stem/progenitor cells (SSPCs) is challenging, I took advantage of the well-established *in vitro* long-term mouse SSPC culture system established in Shanghai Jiao Tong University School of Medicine to explore whether introducing human “smart-and-sex” genes into mouse SSPC could increase the proliferation ability and the stemness of mouse SSPC cells (Figure 19). The cDNAs of eight “smart-and-sex” genes that can enhance the self-renewal of human neural progenitor cells (Figures 16 and 17) were individually cloned into lentivirus vectors containing a green fluorescent protein (GFP) (Figure 19). Then, mouse testicular cells were collected from postnatal day-7 C57BL/6 mice and somatic cells were then removed by overnight attachment to obtain mouse SSPCs (Figure 19). Lentivirus carrying “smart-and-sex” genes was infected into the mouse SSPCs, and cells expressing target genes were enriched via the co-expressed GFP by fluorescence-activated cell sorting (FACS) (Figure 19). The expression effect of “smart-and-sex” genes was evaluated at the protein level using the IF staining assay (Figure 20).

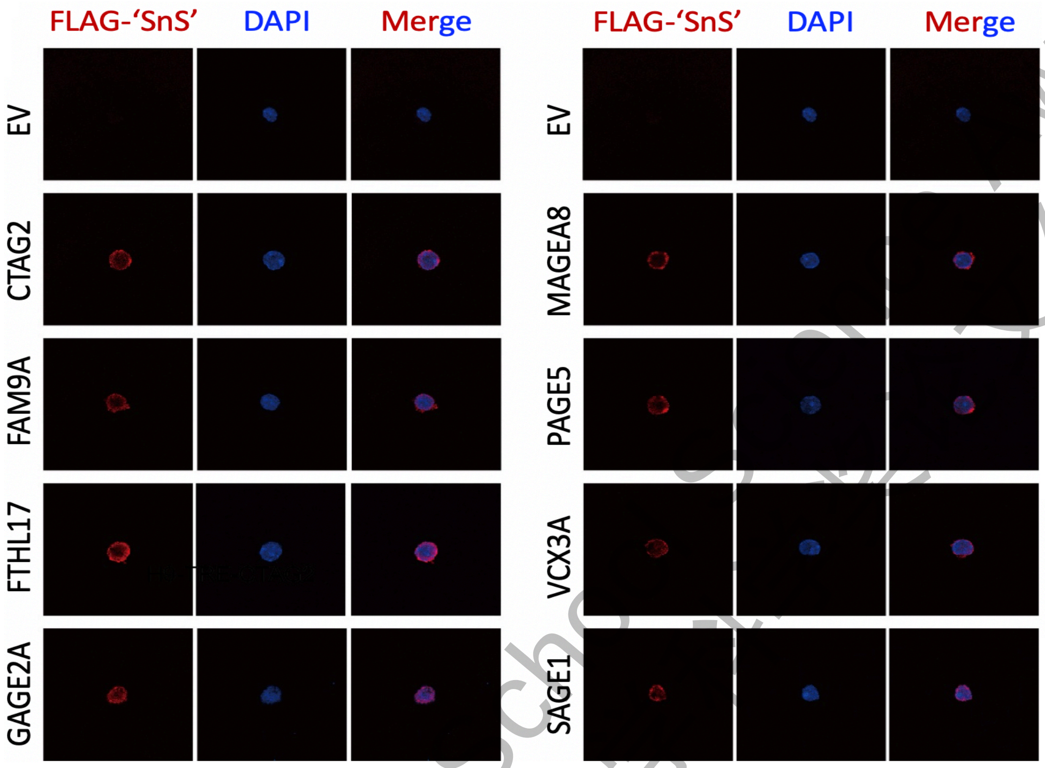

Figure 20. IF analysis shows the expression of Flag-tagged “smart-and-sex” (SnS) genes in mouse SSPCs. “Smart-and-sex” genes were stained by anti-Flag antibody. DAPI signals denote nuclear DNAs. EV: empty vector control.

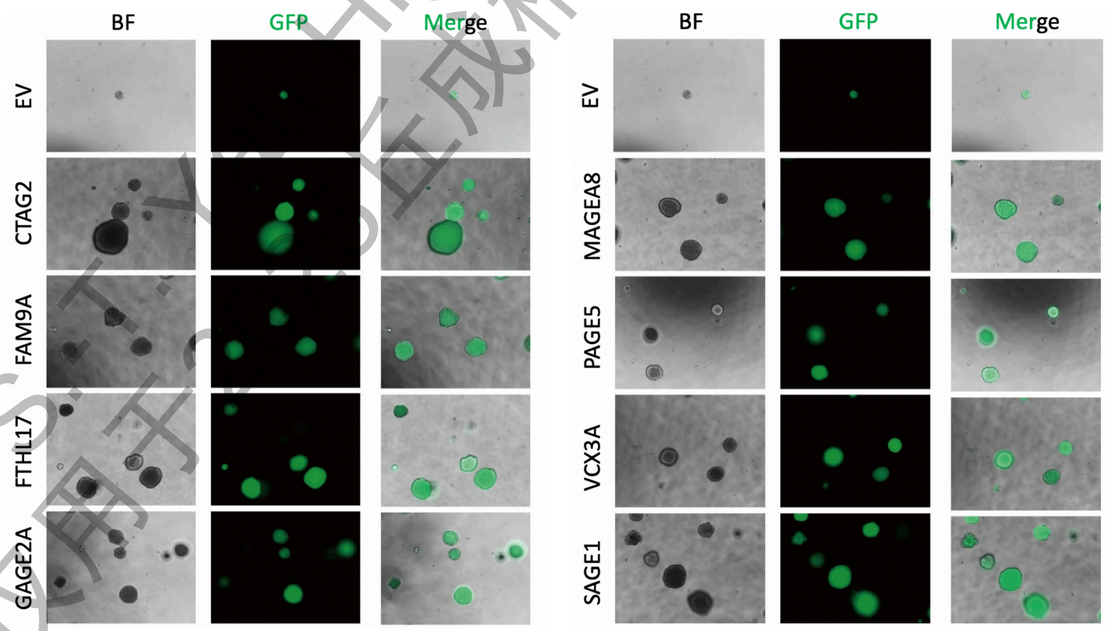

Figure 21. “Smart-and-sex” gene expression in mouse SSPCs leads to much larger SSPC clones than the controls. SSPC clones were visualized via co-expressed GFP using a fluorescent microscope. EV: empty vector control.

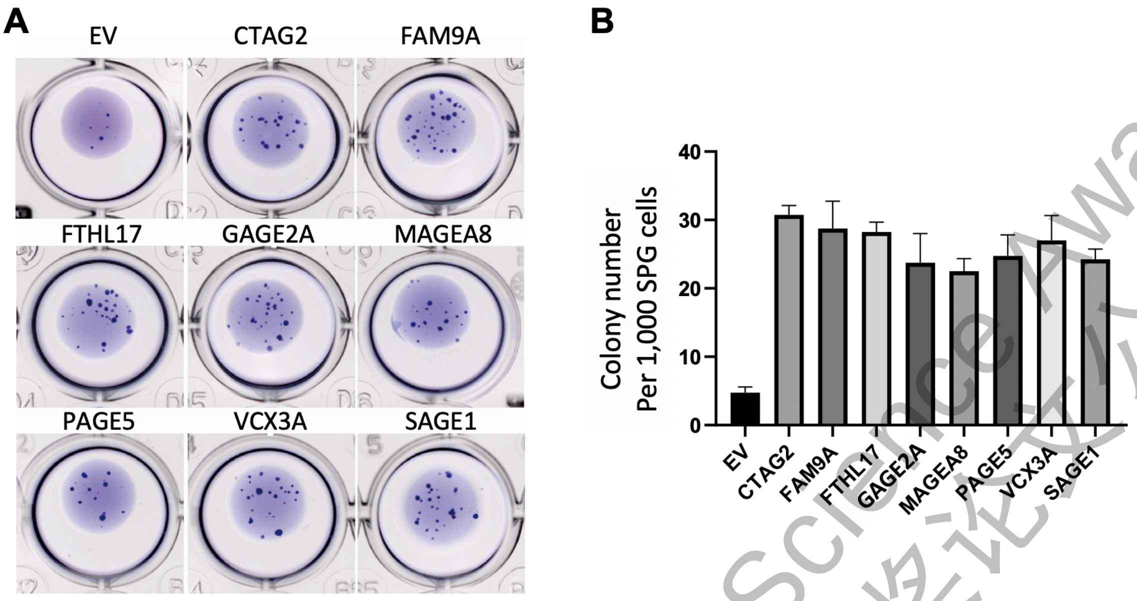

Figure 22. SSPC proliferation to evaluate the "smart-and-sex" genes' function. (A) Colonies of "smart-and-sex" gene-expressing mouse SSPCs in 3D Matrigel were stained with crystal violet. Representative images are shown. EV: empty vector control. **(B)** The quantitation of the colony number per 1,000 SSPCs in "smart-and-sex" gene-expressing SSPCs and the control cells is shown as a bar diagram.

Next, "smart-and-sex" gene-expressing SSPCs were transferred into low attachment wells with Matrigel to form colonies in three-dimensional (3D) cultures (Figure 19). After 35-day growth, the colonies were visualized by GFP under a fluorescent microscope (Figure 21). The 3D culture result revealed that mouse SSPCs transfected with the "smart-and-sex"-gene viruses displayed large 3D spheroids, while mouse SSPCs treated with the empty vector (EV) viruses refrained from amplifying three-

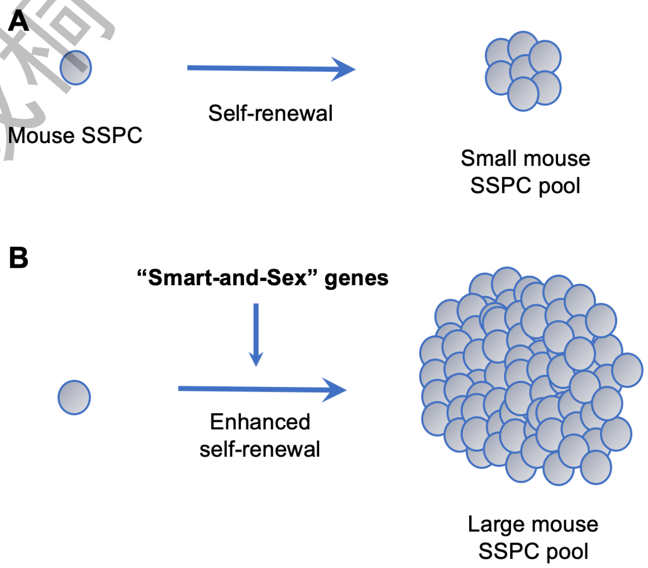

Figure 23. Summary of the results in Section 3.4. "Smart-and-sex" gene expression in mouse SSPCs leads to an enhanced self-renewal ability for mouse SSPCs, giving rise to much larger SSPC clones than the controls.

dimensionally (Figure 21). The 3D spheroids were then fixed and stained with Crystal Violet. Consistent with the 3D spheroid results, the Crystal-Violet-staining data showed that all eight "smart-and-sex" genes function like "*in-vitro* evolved" genes and greatly enhance the self-renewal and proliferation potential of mouse SSPCs (Figure 22).

Taken together, these results provide another strong support for the "smart-and-sex-gene" hypothesis, and demonstrate that the same primate-specific "smart-and-sex" genes that enhance the self-renewal of neural progenitor cells may also play important roles in the self-renewal and long-term maintenance of the large, undifferentiated spermatogonia stem and progenitor pool in primate testis (Figures 18 and 23).

4. DISCUSSION

In this study, I propose the hypothesis that primates have evolved some "smart-and-sex" genes that govern the upgradation of the progenitor cells in both the brain and testis. Through bioinformatic analysis, I identified a group of prospective primate-specific "smart-and-sex" genes with a unique expression pattern that matches both the time of fastest grey matter volume growth rate of infant brain and the period of continuous spermatogenesis in male testis staring from puberty (compare Figures 4 and 5, 6 and 7). Twelve of the "smart-and-sex" genes were selected for functional studies. In human cortical neurogenesis experiments, expression of these genes greatly enhances the self-renewal ability and enlarges the pool of cortical progenitor cells with a slowing down of the differentiation process from progenitor cells to neurons (Figures 16-18). These data demonstrate that the specific expression of the "smart-and-sex" genes during primate cortical neurogenesis provides a mechanistic explanation for why neural progenitors experience a prolonged proliferation process and give rise to an increased cortex size in primates compared to non-primate mammals (Figure 2A). Similarly, introducing these primate-specific "smart-and-sex" genes into mouse spermatogonial stem/progenitor cells (SSPC) induces and thereby mimics an "*in vitro* evolutionary upgradation", leading to a larger pool of SSPC and greatly enhancing their self-renewal and proliferation potential (Figures 2B and 21-23). These data demonstrate that "smart-and-sex" genes are important for both cortical neurogenesis and spermatogenesis in primates, and thus provide a strong support for the "smart-and-sex-gene" hypothesis.

Another interesting finding in this study is that more than a quarter of "smart-and-sex" genes resides in a unique sex chromosome—the X chromosome (Figures 8 and 9). This is not a coincidence. All mammalian males contain two different sex chromosomes, the X and Y chromosomes, whereas females contain a pair of X chromosomes. Therefore the X chromosome in males in fact has been functioning as a "laboratory" to search for "novel genes" with improved characteristics during evolution. The emergence of a group of X-linked, primate-specific "smart-and-sex" genes after the primate-rodent split suggests an increased "efficiency" of this "X-chromosome laboratory". Hence, the emergence of primates must be the result of a joint search for both enhanced brain and testis functions with "smart-and-sex" genes being the evolutionary driving force.

This study leaves some unresolved questions. For example, why is the similarity between brain and the female reproductive organ ovary not as high as the similarity between brain and testis? Won't the "smart-and-sex" genes present in both males and females? Intriguingly, our preliminary bioinformatics analysis suggests that some of the identified "smart-and-sex" genes display an expression peak in human female oogonia cells at about 15-20 weeks post-conception, matching the timing when the oogonia pool undergoes the only round of amplification during the entire female lifetime. This unique expression pattern suggests a potential common mechanism that might govern neural, male and female germ cell development. Further studies will be needed to clarify this common mechanism and explore more secrets about brain, testis, and ovary hidden deep within the human body, at different time points of human development since conception.

Our discoveries presented here will lead to a deeper understanding of the previously underemphasized mechanism underneath neural and germ cell development in primates, and can provide a new direction for future research regarding human physiology and pathology. The "smart-and-sex" genes may be associated with the simultaneous impairment of brain and testis functions. Deeper exploration of these genes and their roles in brain and testis functions could help in better understanding the pathophysiology connection between these two organs, as well as in the development of new therapeutic strategies for treating brain and reproduction related diseases.

5. LIMITATIONS OF THE STUDY

While our study provides new insights into the roles of “smart-and-sex” genes in primate cortical neurogenesis and spermatogenesis, the current bioinformatic analyses and experimental methods have room for improvement. First, the accuracy of the approach I employed for the bioinformatic analysis could be enhanced by more complex analytical methods. In this study, I used the human gene-set as an approximation of the aggregated primate genes, and the sum aggregate of mouse and pig genes as an approximation of the aggregated non-primate mammalian genes. A comprehensive evolutionary dating analysis of all human coding genes could be implemented for an improved accuracy of the primate-specific gene list. Second, the examination of selected “smart-and-sex” gene expression at the protein level was only performed on a human testis sample. Similar experiments for infant brain sample will be needed to fully confirm “smart-and-sex” gene expression at the protein level during brain development. Third, only *in-vitro* cell-based assays were performed to study the functional roles of the “smart-and-sex” genes in cortical neurogenesis and spermatogenesis in the current study. Further *in vivo* investigations, such as human brain organoid and spermatogonia xenotransplantation, are required in the future to fully understand the biological functions of “smart-and-sex” genes in neural and germ cell development in primates.

6. CONCLUSION

Through examining the similarities between primate neural and germ cell development, this paper discusses the important role that primate-specific “smart-and-sex” genes play in enhancing the self-renewal ability and proliferation potential in both cortical neurogenesis and spermatogenesis in primates. The effects that these genes have on the neural and spermatogonial stem/progenitor cells were hypothesized, analyzed using bioinformatic tools performed upon existing human brain and testis transcriptomic data, and verified through *in vitro* cortical neurogenesis and 3D testicular germ cell proliferation experiments. These results support the hypothesis that primates have evolved some “smart-and-sex” genes that govern the advanced traits of the progenitor cells in both the brain and testis. This study will lead to a deeper understanding of the previously underemphasized mechanism underlying neural and germ cell development in primates, and provide a new direction for future research regarding the pathophysiology connection between human brain and testis.

7. REFERENCES

1. Hill, R.S., and Walsh, C.A. (2005). Molecular insights into human brain evolution. *Nature* **437**: 64–67.
2. Amadio, J.P., and Walsh, C.A. (2006). Brain evolution and uniqueness in the human genome. *Cell* **126**: 1033–1035.
3. Silbereis JC, Pochareddy S and Zhu Y et al. (2016) The cellular and molecular landscapes of the developing Human Central nervous system. *Neuron* **89**: 248–68.
4. Molnár Z, Clowry GJ and Šestan N et al. (2019) New insights into the development of the human cerebral cortex. *J Anat* **235**: 432–51.
5. Sousa, A.M.M., Meyer, K.A., Santpere, G., Gulden, F.O., and Sestan, N. (2017). Evolution of the Human Nervous System Function, Structure, and Development. *Cell* 170: 226–247.
6. Lui, J.H., Hansen, D.V., and Kriegstein, A.R. (2011). Development and evolution of the human neocortex. *Cell* **146**: 18–36.
7. Rakic, P. (2009). Evolution of the neocortex: a perspective from developmental biology. *Nat. Rev. Neurosci.* **10**: 724–735.
8. Libe-Philippot B. and Vanderhaeghen P. (2021) Cellular and molecular mechanisms linking human cortical development and evolution. *Annu. Rev. Genet*. **55**:555-81.
9. Zhang R., Quan H., Wang Y., and Luo F. (2023) Neurogenesis in primates versus rodents and the value of non-human primate models. *Natl. Sci. Rev.* **10(11)**: nwad248.
10. Fietz, S.A., Kelava, I., Vogt, J., Wilsch-Bra¨uninger, M., Stenzel, D., Fish, J.L., Corbeil, D., Riehn, A., Distler, W., Nitsch, R., and Huttner, W.B. (2010). OSVZ progenitors of human and ferret neocortex are epithelial-like and expand by integrin signaling. *Nat. Neurosci.* **13**: 690–699.
11. Hansen, D.V., Lui, J.H., Parker, P.R., and Kriegstein, A.R. (2010). Neurogenic radial glia in the outer subventricular zone of human neocortex. *Nature* **464**: 554–561.
12. Pollen AA, Nowakowski TJ, Chen Jet al. (2015) Molecular identity of human outer radial glia during cortical development. *Cell*. **163**: 55–67.
13. Florio M, Albert M and Taverna E et al. (2015) Human-specific gene ARHGAP11B promotes basal progenitor amplification and neocortex expansion. *Science*. **347**: 1465–70.

14. Hou Q-Q, Xiao Q and Sun X-Y et al. (2021) TBC1D3 promotes neural progenitor proliferation by suppressing the histone methyltransferase G9a. *Sci Adv* **7**: eaba8053.
15. Suzuki IK, Gacquer D and Van Heurck R et al. (2018) Human-specific NOTCH2NL genes expand cortical neurogenesis through delta/notch regulation. *Cell* **173**: 1370–84.
16. Van Heurck R, Bonnefont J and Wojno M et al. (2023) CROCCP2 acts as a human-specific modifier of cilia dynamics and mTOR signaling to promote expansion of cortical progenitors. *Neuron* **111**: 65–80.
17. Heide M, Haffner C and Murayama A et al. (2020) Human-specific ARHGAP11B increases size and folding of primate neocortex in the fetal marmoset. *Science* **369**: 546–50.
18. Kalebic N, Gilardi C and Albert M et al. (2018) Human-specific ARHGAP11B induces hallmarks of neocortical expansion in developing ferret neocortex. *Elife* **7**: e41241.
19. Liu J, Liu W and Yang L et al. (2017) The primate-specific gene TMEM14B marks outer radial glia cells and promotes cortical expansion and folding. *Cell Stem Cell*. **21**: 635–49.
20. Espuny-Camacho, I., Michelsen, K.A., Gall, D., Linaro, D., Hasche, A., Bonne-font, J., Bali, C., Orduz, D., Bilheu, A., Herpoel, A., et al. (2013). Pyramidal neurons derived from human pluripotent stem cells integrate efficiently into mouse brain circuits in vivo. *Neuron* **77**: 440–456.
21. Guo J., Zhu P., Wu C., Yu L., Zhao S., Gu X. (2003) In silico analysis indicates a similar gene expression pattern between human brain and testis. *Cytogenet. Genome Res*. **103**: 58–62.
22. Guo J.H., Huang Q., Studholme D.J., Wu C.Q., and Zhao S.Y. (2005) Transcriptomic analyses support the similarity of gene expression between brain and testis in human as well as mouse. *Cytogenet. Genome Res*. **111**: 107–109.
23. Matos B., Publicover S. J., Castro L.F.C., and Esteves P.J. (2021) Fardilha M. Brain and testis: more alike than previously thought? *Open Biology* **11**: 200322.
24. Arden R., Gottfredson L.S., Miller G., and Pierce A. (2009) Intelligence and semen quality are positively correlated. *Intelligence* **37**: 277–282.
25. Fayomi, A.P. and Orwig K.E. (2018) Spermatogonial stem cells and spermatogenesis in mice, monkeys and men. *Stem Cell Research*. **29**: 207-14.
26. Sharma S., Wistuba J., Pock T., Schlatt S., and Neuhaus N. (2019) Spermatogonial stem cells: updates from specification to clinical relevance. *Hum. Reprod. Update*. **25(3)**:275-97.

27. Phillips, B.T., Gassei, K., and Orwig, K.E. (2010) Spermatogonial stem cell regulation and spermatogenesis. *Philos. Trans. R. Soc. Lond. Ser. B Biol. Sci.* **365**: 1663–1678.
28. de Rooij, D.G. and Grootegoed, J.A. (1998) Spermatogonial stem cells. *Curr. Opin. Cell Biol.* **10**: 694–701.
29. Tegelenbosch, R.A. and de Rooij, D.G. (1993) A quantitative study of spermatogonial multiplication and stem cell renewal in the C3H/101 F1 hybrid mouse. *Mutat. Res.* **290**: 193–200.
30. Clermont, Y. (1966) Renewal of spermatogonia in man. *Am. J. Anat*. **118**: 509–524.
31. Schulze, W. (1978) Light and electron microscope studies of the morphology of A spermatogonia in men with normal spermatogenesis and in patients treated with anti-androgens. *Andrologia* **10**: 307–320.
32. Paniagua, R., Codesal, J., Nistal, M., Rodriguez, M.C., and Santamaria, L. (1987) Quantification of cell types throughout the cycle of the human seminiferous epithelium and their DNA content. A new approach to the spermatogonial stem cell in man. *Anat. Embryol.* **176**: 225–230.
33. Marshall, G.R. and Plant, T.M. (1996) Puberty occurring either spontaneously or induced precociously in rhesus monkey (Macaca mulatta) is associated with a marked proliferation of Sertoli cells. *Biol. Reprod*. **54**: 1192–1199.
34. Anand S., Patel H., and Bhartiya D. (2015) Chemoablated mouse seminiferous tubular cells enriched for very small embryonic-like stem cells undergo spontaneous spermatogenesis in vitro. *Reprod Biol Endocrinol* **13**:33.
35. Sakib S., Yu Y., Voigt A., Ungrin M., and Dobrinski I.(2019) Generation of Porcine Testicular Organoids with Testis Specific Architecture using Microwell Culture. *J Vis Exp.* **152**: e60387.
36. Bethlehem R.A.I., et al. (2022) Brain charts for the human lifespan. *Nature.* **604(7906)**: 525-33.
37. Cardoso-Moreira M., et al. (2019) Gene expression across mammalian organ development. *Nature.* **571(7766)**: 505-9.
38. Koskenniemi, J.J., Virtanen, H.E., and Toppari J. (2017) Testicular growth and development in puberty. *Curr Opin Endocrinol Diabetes Obes.* **24(3)**:215-224.

8. ACKNOWLEDGMENTS

To me, biology, chemistry, physics, and even philosophy are all interrelated. What makes human beings what we are today? What makes humans intelligent? These questions have always intrigued me. I started to seek answers in IB Biology and participated in Biology Olympiads and iGEM research while studying *Being Human* in IB philosophy. Later, through my biology teacher, Mr. Hui Liao, I learned about a research opportunity for humans' "smart gene" at Shanghai Jiao Tong University School of Medicine. It immediately caught my attention, and I eagerly embarked on the hands-on experimental journey of life science. In the lab, I started by looking into the brain-testis similarities, an area that anyone who studies the brain wouldn't miss. The observation of some common characteristics of progenitor cells in the human brain and testis makes me wonder if there exist some "smart-and-sex" genes that could explain the similarities and contribute to human development of the advanced cognitive and reproductive traits. In fact, the "smart genes" I have been chasing turned out to be something even smarter, multi-tasking "smart-and-sex" genes.

I extend my deepest gratitude to my mentors, Dr. Yanjie Zhang from Shanghai Jiao Tong University School of Medicine and Teacher Hui Liao from Shanghai High School International Division, who guided me through the entire project. They provided me with background knowledge, brainstormed with me about project ideas, and advised me on the research direction. Both Dr. Zhang and Teacher Liao made valuable suggestions to the final research essay writing, from structure, use of terminology, to the final data presentation. Dr. Zhang also taught me how to set up the research plan and how to design both bioinformatics dry-lab experiments and cell-based wet-lab functional experiments. During the experimentation, I encountered many puzzling moments, and Dr. Zhang guided me to overcome the challenges. One that stood out, for example, is that at first, I couldn't see any meaningful pattern when only adult brain transcriptome data was used to search for the potential "smart-and-sex" genes. Thanks to several rounds of discussion with Dr. Zhang, I realized I should include human brain transcriptomic data obtained from samples covering all developmental stages of the human brain, including the infant stage, which finally yielded the list of "smart-and-sex" genes.

I'm grateful to Dr. Qin Yang, the research assistant in Dr. Zhang's team, who taught me how to obtain useful datasets, how to add the target genes in plasmids using SnapGene, and how to use the puromycin antibiotic as a selection mechanism to express "smart-and-sex" genes. I also want to thank Drs. Guo and Wei, research associates in the lab, who taught me how to perform cellular assays in cortical neurogenesis and spermatogenesis, including numerous molecular and cellular biology techniques, such as stem cell culture, lentivirus preparation and infection, immunohistochemistry and immunofluorescence staining, flow cytometry, and 3D spheroid formation assay. Without their help, I couldn't imagine getting this far.

Through this project, not only did I find out more about human development, but I also became excited to have embarked on a journey towards discovering novel genes that could contribute to potential therapeutics of neural and reproductive diseases.